Inactivation of Bacterial DD-Peptidase by β-Sultams†

Antonio Llinás,‡ Naveed Ahmed,‡ Massimiliano Cordaro,‡ Andrew P. Laws,‡ Jean-Marie Frère,§ Michael Delmarcelle,§ Nicholas R. Silvaggi,‖ Judith A. Kelly,‖ and Michael I. Page*,‡

Department of Chemical and Biological Sciences, The University of Huddersfield, Huddersfield HD1 3DH, U.K., Centre d'Ingénierie des Protéines, Institut de Chimie B6, Sart-Tilman, B-4000 Liège 1, Belgium, and Department of Molecular and Cell Biology and Institute for Materials Science, University of Connecticut, Storrs, Connecticut 06269-3125

Received January 19, 2005; Revised Manuscript Received April 7, 2005

ABSTRACT: *N*-Acyl-β-sultams are time-dependent, irreversible active site-directed inhibitors of *Streptomyces* R61 DD-peptidase. The rate of inactivation is first order with respect to β-sultam concentration, and the second-order rate constants show a dependence on pH similar to that for the hydrolysis of a substrate. Inactivation is due to the formation of a stable 1:1 enzyme−inhibitor complex as a result of the active site serine being sulfonylated by the β-sultam as shown by ESI-MS analysis and by X-ray crystallography. A striking feature of the sulfonyl enzyme is that the inhibitor is not bound to the oxyanion hole but interacts extensively with the "roof" of the active site where the Arg 285 is located.

D-Alanyl-D-alanine carboxypeptidase/transpeptidases [DD-peptidases and also known as penicillin-binding proteins, or PBPs (*1*)] are enzymes produced by bacteria that catalyze the final steps of their cell wall biosynthesis (*1*, 2). Bacteria, with a very few exceptions, have a cross-linked cell wall, the formation of which involves a transpeptidation reaction that is catalyzed by bacterial transpeptidases/PBPs. The PBPs have been classified into two groups: the low molecular mass (LMM) PBPs and the high molecular mass (HMM) PBPs (*3*). The low molecular mass group includes β-lactamases that catalyze the hydrolysis of β-lactam antibiotics, the D-Ala-D-Ala carboxypeptidases, and endopeptidases. The HMM PBPs catalyze the transpeptidation reaction that cross-links the glycan strands of the cell wall (*3*, *4*).

The DD-peptidases are the inhibition targets of β-lactam antibiotics, such as penicillin and cephalosporins. These enzymes have an active site serine residue that is acylated by the D-Ala-D-Ala natural peptide substrate as an intermediate stage of the acyl transfer reaction (*5*) (Scheme 1). The β-lactam antibiotics act as mechanism-based inhibitors for the PBPs by acting as substrates for nucleophilic attack by the active site serine causing C−N bond fission and ring opening to form stable acyl-enzyme intermediates that are then not susceptible to further nucleophilic attack by exogenous amines or water (Scheme 2). Deacylation is very slow because the leaving amino group remains covalently attached to the acyl-enzyme and presumably blocks nucleophilic attack by the amino group of the acceptor or by water (*6*).

Bacterial resistance to β-lactam antibiotics has emerged primarily through two mechanisms: the production of β-lactam degrading enzymes, the β-lactamases, and the accumulation of mutations in their HMM PBP targets which

Scheme 1

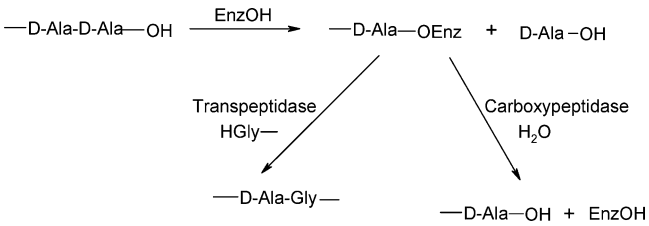

Scheme 2

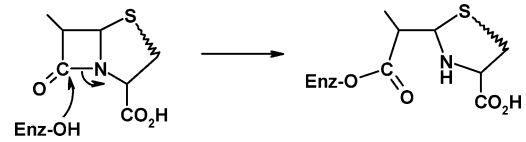

render them less susceptible to inhibition by β-lactam antibiotics. The most important defense mechanism is the production of β-lactamases [thought to be evolutionary descendants of DD-peptidases (*3*−*7*)]. Some of the β-lactamases are serine enzymes and also catalyze the hydrolysis of β-lactams through the formation of an acyl-enzyme but, in this case, to give a short-lived intermediate that is quickly hydrolyzed before the β-lactams can reach their transpeptidase or DD-peptidase targets.

The DD-peptidase of *Streptomyces* R61 is secreted in the extracellular medium as a soluble protein and catalyzes the cleavage of the C-terminal D-alanine of simple synthetic peptides. In the presence of acceptor compounds having a suitably located amino group, they also perform transpeptidation reactions (Scheme 1) (*8*, *9*). The specificity of the enzymes for the acceptors reflects the structure of the bacteria's peptidoglycan cross-bridges, and for *Streptomyces* R61 DD-peptidase, dipeptides, such as Gly-L-Ala, are good acceptors. The R61 enzyme is a 37.5 kDa enzyme (EC 3.4.16.4) that has 349 residues and has been used extensively as a kinetic and structural model for PBPs (*9*, *10*). The use of ester and thiolester substrates for the DD-peptidases

† This research was supported by the University of Huddersfield.
* To whom correspondence should be addressed: phone, +1484 472169; fax, +1484 472182; e-mail, m.i.page@hud.ac.uk.
‡ The University of Huddersfield.
§ Institut de Chimie B6.
‖ University of Connecticut.

10.1021/bi050110o CCC: $30.25 © 2005 American Chemical Society
Published on Web 05/07/2005

Chart 1

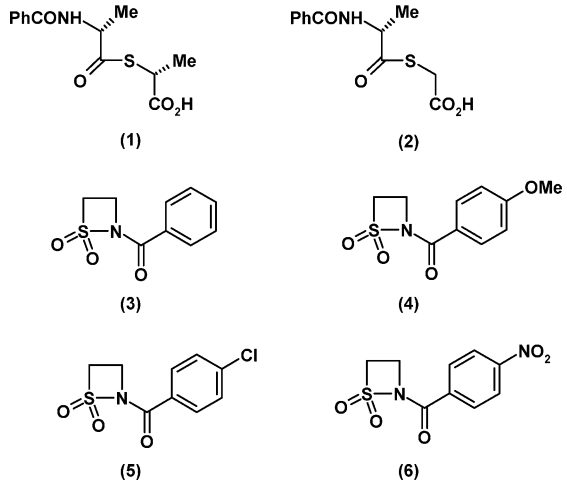

Scheme 3

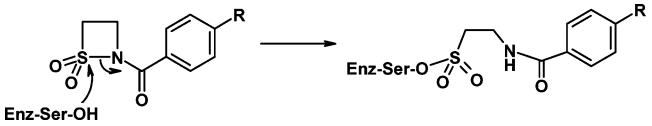

represented a significant advance in the study of their reactions. The study of thioesters as substrates can be followed by spectrophotometry, allowing a continuous monitoring of enzyme activity. Moreover, with the thioester substrates, deacylation is rate-limiting with several enzymes, so that the complete catalytic pathway could be more easily studied (*11*). In this study *N*-benzoyl-D-Ala-thiolactate (**1**) and *N*-benzoyl-D-Ala-thioglycolate (**2**) (see Chart 1) were synthesized and used as substrates to monitor the activity of *Streptomyces* R61.

The continued efficiency of β-lactam antibiotics is increasingly compromised by the ability of bacteria to produce more and more β-lactamases. The present strategy to overcome this problem is to use a combination of a β-lactam antibiotic and an inhibitor of β-lactamase. Ideally, it would be useful to have a single drug which inhibited both the transpeptidases and the β-lactamases. This has already been reported using boronic acids (*12*) and phosphonates (*13*).

β-Sultams (1,2-thiazetidine 1,1-dioxides) are cyclic sulfonamides and the sulfonyl analogues of β-lactams. Sulfonamides have not been explored as potential sulfonylating agents of enzymes because of their general low reactivity. However, we have shown (*14*) that the reactivity of β-sultams contrasts strongly with that of their acyclic sulfonamide counterparts (ca. 10^8-fold more reactive) and is even 10^2–10^3-fold more reactive than the corresponding β-lactams. We have shown that β-sultams are inhibitors of a serine β-lactamase (*15*) as well as the serine protease elastase (*16*) and that this is due to sulfonylation of the active site serine (Scheme 3). Herein we report the inhibitory properties of β-sultams with *Streptomyces* R61 DD-peptidase. Crystallography has been useful for observing substrates and inhibitors covalently bound to DD-peptidases (*17*–*20*); however, the efficiency of substrate hydrolysis in the R61 crystals has made the observations of substrate analogues difficult.

EXPERIMENTAL PROCEDURES

Materials. Streptomyces sp. R61 DD-peptidase was prepared as described previously (*21*) and used as a 0.5 mg/mL aqueous solution in 10 mM Tris buffer, pH 8. AnalaR grade reagents were purchased from Sigma, and deionized water was used throughout.

Methods. HPLC experiments were carried out in a Beckmann System Gold model 127 pump and model 168 diode array detector fitted with a Lichospher 100RP-18, 5 mm, column. The solvent was 5% H_2O (1% TFA)/CH_3CN, flow = 0.5 mL/min, and λ = 230 nm. ESIMS experiments were carried out on a VG Quattro SQ II (Micromass, Altrincham, England). ^{1}H NMR and ^{13}C NMR experiments were carried out on a Bruker 400 MHz (Rheinstetten, Germany). Standard UV spectroscopy was carried out on a Cary 1E UV–visible spectrophotometer (Varian, Mulgrave, Australia) equipped with a 12-compartment cell block. The instrument was used in double beam mode, allowing six reaction cells to be followed in single run. The cell block was thermostated using a peltier system.

Synthesis. The synthesis of *N*-benzoyl-D-Ala-thio-D-lactate (**1**) and *N*-benzoyl-D-Ala-thioglycolate (**2**) is described in the Supporting Information. Taurinesulfonyl chloride, 1,2-thiazetidine 1,1-dioxide, and 2-benzoyl-1,2-thiazetidine 1,1-dioxide (**3**) were prepared as previously described (*22*).

*2-(4′-Methoxybenzoyl)-1,2-thiazetidine 1,1-Dioxide (**4**).* 4-Methoxybenzoyl chloride (1.59 g, 9.32 mmol) was added dropwise to a solution of 1,2-thiazetidine 1,1-dioxide (1 g, 9.33 mmol) and DMAP (0.2 g) in anhydrous DCM (50 mL) at −78 °C. The reaction mixture was stirred for 30 min before triethylamine (0.94 g, 9.29 mmol) was added dropwise over 10 min at −78 °C forming a white precipitate. The mixture was then allowed to stir at room temperature for 24 h before the reaction mixture was filtered and the solvent removed by reduced pressure rotary evaporation at 30 °C. The colorless oil was purified using column chromatography (silica, 50 g) (3:2 ether:DCM): R_f = 0.35 (1.2 g, 53%); mp 98–99 °C; IR (neat, ν, cm^{-1}) 3035, 2977, 2841, 1662, 1606, 1513, 1327, 1262, 1201, 1156, 1031; ^{1}H NMR (δ, ppm, $CDCl_3$) 8.01 (2H, d, J = 8.95 Hz, Ha/Hc), 7.01 (2H, d, J = 8.87 Hz, Hb/Hd), 4.27 (2H, t, J = 7.35 Hz, CH_2SO_2), 3.98 (2H, t, J = 7.22 Hz, CH_2–N), 3.88 (H, s, CH_3); ^{13}C NMR (δ, ppm, $CDCl_3$) 163.95 (CO), 132.25 [quaternary carbon (1)], 130.87 (CH a/c), 124.26 [quaternary carbon (2)], 114.22 (CH b/d), 55.56 (CH_2–SO_2), 55.45 (CH_3), 30.72 (CH_2–N); HREI-MS [M + H]$^+$ for $C_9H_9NO_3S$ calculated, 242.2734; measured, 242.2732.

*2-(4′-Chlorobenzoyl)-1,2-thiazetidine 1,1-Dioxide (**5**).* 4-Chlorobenzoyl chloride (1.63 g, 9.31 mmol) was added dropwise to a solution 1,2-thiazetidine 1,1-dioxide (1 g, 9.33 mmol) and DMAP (0.2 g, 1.63 mmol) in anhydrous dichloromethane (50 mL) at −78 °C. The reaction mixture was stirred for 30 min before triethylamine (1.2 mL, 9.31 mmol) was added dropwise over 10 min at −78 °C, forming a white precipitate. The mixture was allowed to stir at room temperature for 24 h before the reaction mixture was filtered and the solvent removed by rotary evaporation at 30 °C. The pale yellow oil was purified by column chromatography (3:2 ether:DCM): R_f = 0.57 (0.89 g, 39%); mp 84–86 °C; IR (neat, ν, cm^{-1}) 1676, 1593, 1404, 1357, 1323, 1159, 1092, 1016; ^{1}H NMR (δ, ppm, $CDCl_3$) 7.96 (2H, d, J = 8.64 Hz,

Ha/Hc), 7.51 (2H, d, $J = 8.69$ Hz, Hb/Hd), 4.33 (2H, t, $J = 7.10$ Hz, CH_2SO_2), 3.93 (2H, t, $J = 7.07$ Hz, CH_2N); ^{13}C NMR (δ, ppm, $CDCl_3$) 166.2 (C=O), 140.2 [quaternary carbon (1)], 134.5 [quaternary carbon (2)], 129.85 (CH a/c), 129.34 (CH b/d), 57.0 (CH_2SO_2), 30.9 (CH_2N); HREI-MS (EI) for $C_9H_8ClNO_3S$ calculated, 244.9908; measured, 244.9905.

*2-(4′-Nitrobenzoyl)-1,2-thiazetidine 1,1-Dioxide (**6**).* 4-Nitrobenzoyl chloride (1.73 g, 9.32 mmol) was added dropwise to a solution of 1,2-thiazetidine 1,1-dioxide (1 g, 9.33 mmol) and DMAP (0.2 g, 1.63 mmol) in anhydrous dichloromethane (50 mL) at −78 °C. The reaction mixture was stirred for 30 min before triethylamine (1.3 mL, 9.29 mmol) was added dropwise over 10 min at −78 °C, forming a white precipitate. The mixture was allowed to stir at room temperature for 24 h before the reaction mixture was filtered and the solvent removed by rotary evaporation at 30 °C. The colorless oil was purified by column chromatography (silica, 35 g) (3:2 hexane:EtOAc): $R_f = 0.28$ (0.82 g, 34%); mp 90−92 °C; IR (neat, ν, cm^{-1}) 3114, 3057, 1664, 1604, 1521, 1347, 1324, 1284, 1215, 1164; ^1H NMR (δ, ppm, $CDCl_3$) 8.27 (2H, d, $J = 8.86$ Hz, Hb/Hd), 8.06 (2H, d, $J = 8.83$ Hz, Ha/Hc), 4.37 (2H, t, $J = 7.15$ Hz, CH_2SO_2), 3.88 (2H, t, $J = 7.22$ Hz, CH_2N); ^{13}C NMR (δ, ppm, $CDCl_3$) 165.88 (C=O), 149.98 [quaternary carbon (2)], 137.14 [quaternary carbon (1)], 129.02 (CH b/d), 123.45 (CH a/c), 57.34 (CH_2SO_2), 30.86 (CH_2N); HREI-MS (EI) for $C_9H_8N_2O_5S$ calculated, 256.0148; measured, 256.0151.

Kinetics Studies. (a) Nonenzyme-Catalyzed Hydrolysis. The rate of hydrolysis of *N*-benzoyl-β-sultam (**3**) was obtained spectrophotometrically by following the absorbance decrease at 250 nm as a function of time at 30 °C, $I = 1.0$ mol dm^{-3} (KCl), in 5% MeCN (v/v). For solution pHs ≥3 and ≤11 the pH was controlled by the use of 0.1 mol dm^{-3} buffer solutions. The following buffers were used: sodium formate (pK_a 3.75), sodium acetate (pK_a 4.72), MES (pK_a 6.1), MOPS (pK_a 7.2), TAPS (pK_a 8.4), CAPSO (pK_a 9.6), and CAPS (pK_a 10.4). Buffers were prepared by partial neutralization of solutions of their sodium salts to the required pH.

The rates of hydrolysis of the thioester substrates were followed by measuring the decrease in absorbance at 285 nm for Bz-D-Ala-thioglycolate (**2**) and at 280 nm for Bz-D-Ala-thio-D-lactate (**1**), as a function of time at 30 °C and $I = 1.0$ mol dm^{-3} (KCl). Generally, 10 μL of a stock solution of substrate (0.08 mol dm^{-3} in dry acetonitrile) was injected into 2.0 mL of buffer solution (0.01−0.10 mol dm^{-3}) to give a concentration in the assay cell of 4×10^{-4} mol dm^{-3}. Hydroxide ion concentrations were calculated from the measured pH and using p$K_w(H_2O) = 13.83$ at 30 °C (*23*).

*(b) R61-Catalyzed Hydrolysis of Bz-D-Ala-thioglycolate (**2**) and Bz-D-Ala-thio-D-lactate (**1**).* Generally, 25 μL of a stock solution of thioester substrate was injected into 2.5 mL of buffer solution [0.05 mol dm^{-3}, 30 °C, and $I = 1.0$ mol dm^{-3} (KCl)] followed by 25 μL of a stock solution of enzyme. Usually, the substrate and enzyme concentrations in the cell were 8×10^{-4} mol dm^{-3} and 3.3×10^{-8} to 1.8×10^{-7} mol dm^{-3}, respectively. Hydrolysis of the substrates was followed by measuring the decrease in absorbance at 285 nm for Bz-D-Ala-thioglycolate (**2**) and at 280 nm for Bz-D-Ala-thio-D-lactate (**1**), as a function of time. The kinetic constants were generally determined by following the entire first-order course of the reaction (5−10 half-life times). Complete time curves were studied because of increased accuracy, and there was no evidence of product inhibition or enzyme denaturation. Repeat kinetic runs, performed by injecting more substrate into the cell after the first reaction was complete, gave identical rate constants. Furthermore, rate constants obtained from initial rate studies also gave the same rate constants. The rate constants have an estimated error of ±3%. Curve fittings were achieved using SCIENTIST (MicroMath Scientific Software, St. Louis, MO) software.

*(c) Inhibition of Streptomyces R61 by N-Aroyl-β-sultams (**3**−**6**).* Twenty microliters of a stock solution of the *N*-aroyl-β-sultam (1.24×10^{-2} mol dm^{-3} in dry acetonitrile) were injected into 2.0 mL of buffer solution (MES, pH = 5.96, $I = 0.1$ mol dm^{-3}) to give concentrations of β-sultam in the assay cells of $1.10-1.30 \times 10^{-4}$ mol dm^{-3}. Hydroxide ion concentrations were calculated from the measured pH and using p$K_w(H_2O) = 13.83$ at 30 °C (*23*).

In a typical time-dependent inhibition experiment, an incubation cell ([R61] = 3.85×10^{-7} mol dm^{-3}, [β-sultam] = 2.29×10^{-4} mol dm^{-3} in MES buffer, pH = 5.96) at 30 °C and 50 μL were injected at different time intervals into 2 mL of MOPS buffer, pH = 7.00, containing a thioester (Bz-D-Ala-thioglycolate = 2.02×10^{-4} mol dm^{-3}) to measure enzyme activity. Control experiments were performed in the absence of β-sultam. Because the concentration of the enzyme is much lower than that of the inhibitor at time zero, the inactivation reaction is effectively pseudo first order. To take into account the competing hydrolysis reaction at high pH, the results were normalized with respect to the decreasing β-sultam concentration due to hydrolysis. Because the competing alkaline hydrolysis reaction reduces the concentration of the inhibitor present with time, it consequently reduces the rate of the enzyme inactivation. To correct for this, the results of the inactivations were normalized with respect to the decreasing β-sultam concentration using the equation:

$$\text{normalized rate at time } t = (\text{observed rate}/[\text{sultam}]_o)[\text{sultam}]_t$$

(d) X-ray Crystallographic Studies. The R61 DD-peptidase was crystallized using the hanging drop vapor diffusion method as described in ref *24*. The covalent complex with **3** was obtained by soaking a 0.35 × 0.2 × 0.1 mm crystal in a saturated (<10 mM) solution of **3** in 30% poly(ethylene glycol) (PEG) 8000, 50 mM sodium phosphate, pH 6.8, and 5% (w/v) glycerol for 1 h. Before mounting, the crystal was transferred into a fresh drop of the soak solution containing 10% glycerol and then into a third drop containing 20% glycerol. The crystal was then flash-cooled in a gaseous nitrogen stream at 100 K. Data were collected on beamline X25 at the National Synchrotron Light Source (NSLS), Brookhaven National Laboratory, Upton, New York, and processed using the HKL package (*25*). Statistics for the data collection are provided in Table 1.

Initial phases were derived from the native R61 DD-peptidase structure (PDB ID 3PTE). The crystallographic model was refined using the program CNS (*26*) against data to 1.5 Å resolution. Solvent molecules having reasonable hydrogen bond distances and geometry were added, taking care to avoid modeling the electron density of the bound

Table 1: Crystallographic Data for the Complex with *N*-Benzoyl-β-sultam (**3**)

resolution limit (Å)	1.05
no. of reflections	
measured	1217198
unique	152562
reflections, $F > 4\sigma$	133622
completeness (%)	
all data	95.9
highest resolution shell	84.4
R_{sym}* (on I)	
all data	0.069
highest resolution shell	0.311
$I/\sigma(I)$	
all data	30.5
highest resolution shell	4.9
refinement	
resolution (Å)	10−1.05
R_{cryst} (all data)	0.114
R_{free}	0.136
data in test set	7557
non-hydrogen atoms	3096
rms deviations	
bond lengths (Å)	0.014
angles (deg)	0.98
average B factor (all atoms) (Å^2)	12.4
average B factor of **3** (covalent)[a] (Å^2)	14.7
average B factor of **3** (noncovalent)[a] (Å^2)	12.2

[a] There are two molecules of **3** in this structure. One is bound covalently to Ser 62 Oγ, while the other makes fortuitous interactions with a region of the active site involved in recognition of the natural cell wall peptide.

inhibitor as solvent. Once the refinement converged (R_{cryst} = 0.205, R_{free} = 0.211), the model was refined further using SHELX-97 (*27*). After isotropic refinement to the full resolution, 1.05 Å, anisotropic displacement parameters were refined for all non-hydrogen atoms. Anisotropic refinement resulted in a 4.0% drop in R_{free}. Iterative cycles of fitting in XtalView (*28*) followed by refinement in SHELXL continued until the R factors converged at 0.120 and 0.145. At this point, all hydrogens except those in methyl and hydroxyl groups were added to the model using the riding model in SHELXL. Adding hydrogen atoms resulted in a 0.9% drop in R_{free}.

RESULTS AND DISCUSSION

pH−Rate Profile for the R61-Catalyzed Hydrolysis of Thioester Substrates. The total reaction profile for the hydrolysis of the thioesters (**1** and **2**) catalyzed by R61 was followed to give pseudo-first-order rate constants k_{obs} that were proportional to enzyme concentration. No effective saturation of the enzyme-catalyzed reaction was observed at substrate concentrations up to 2 mM. Hence, it was not possible to obtain reliable values for k_{cat} and K_m. Plotting the rate constants k_{obs} against the enzyme concentration gave the second-order rate constants k_{cat}/K_m which at pH 7 were 5.04×10^3 M^{-1} s^{-1} for **1** and 1.38×10^4 M^{-1} s^{-1} for **2**. It is evident from these values that although the thioesters (**1** and **2**) are convenient for UV assays of R61, they are only moderately good substrates for an "activated" derivative. The estimated K_m values are relatively high, indicating a poor degree of enzyme−substrate binding. The activity of R61 was determined in buffer solutions of pH 4−9, and Figure 1 shows the dependence of k_{cat}/K_m upon pH for hydrolysis of the thioester substrate (**2**) catalyzed by R61 at 30 °C and I = 1.0 M (KCl) at various pHs.

The pH−rate profile indicates that a single ionization of pK_a 4.99 ± 0.09 determines enzyme activity and that this

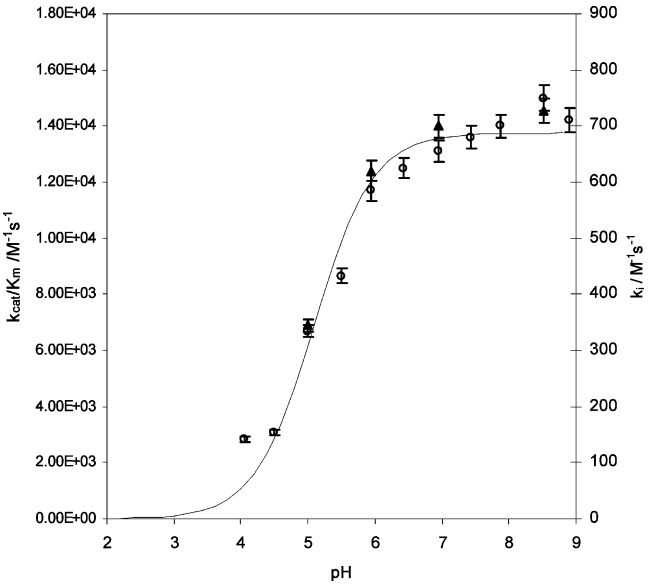

FIGURE 1: Second-order rate constants (k_{cat}/K_m) (○) for the hydrolysis of Bz-D-Ala-thioglycolate catalyzed by *Streptomyces* R61 as a function of pH. Also shown are the second-order rate constants k_i (▲) for the inhibition of R61 by *N*-benzoyl-β-sultam. Rate constants were measured at 30 °C and I = 1.0 mol dm^{-3} (KCl) and have an estimated error of ±3%.

acid group needs to be in its deprotonated form for maximum enzyme activity. There is no evidence of other ionizable and catalytically important groups, and the enzyme activity is characterized by a large pH-independent region from pH 6 to pH 9. Similar observations were seen with the thioester substrate (**1**).

The low pK_a of 5.0 could be due to the ionization of a carboxylic acid residue, but there appears to be no such residue in the active site, so this may reflect a base with a severely reduced pK_a. Possible candidates are Lys 65 or Tyr 159, which are placed at an adequate distance (Figure 3) and are capable of acting as a general base catalyst for the acylation step. These residues have been previously suggested to act as general base catalysts (*20*, *29*, *30*), but without knowledge of the pK_a. A pK_a of 5.0 would be an extraordinary reduction in the base strength of either a lysine or tyrosine residue. An alternative explanation is that the pK_a might reflect the deprotonation of the carboxylate on the substrates used in these studies. However, this is high for such a carboxylic acid, which would be expected to have a pK_a of about 3.5. It has been observed that the K_m for a peptide substrate increased going from pH 6 to pH 5 (*31*), but unfortunately, the study did not extend below pH 5. It is notable that effective β-lactams generally possess a carboxylate that binds in the active site in a position similar to that of the carboxylate of peptide substrates. Enhanced substrate binding due to ionization should be characterized by a lower K_m value, but the K_m values were experimentally inaccessible in these studies.

Inactivation of R61 by β-Sultams. To test the inhibitory properties of *N*-acyl-β-sultams with respect to R61, the enzyme and β-sultam were incubated together in a buffered solution that was referred to as the incubation cell. Aliquots of the incubation solution containing enzyme and β-sultam were then removed from the incubation cell after time t and assayed for enzyme activity against the thioester substrate (**2**) in separate assay cells at pH 6. These assays showed a

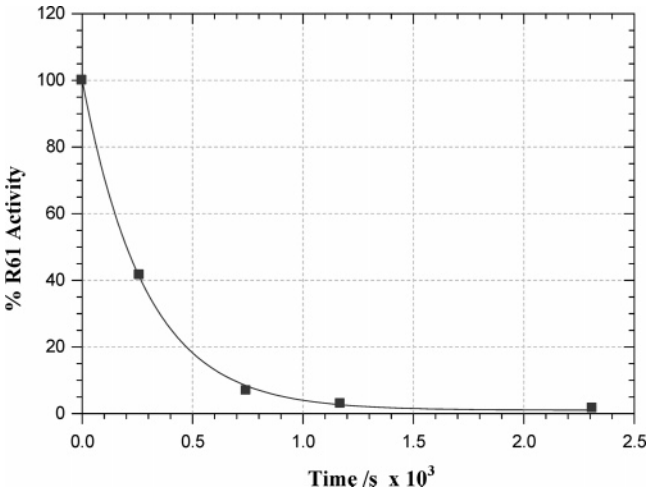

FIGURE 2: Plot of percent activity of *Streptomyces* R61 against incubation time for the inactivation of DD-peptidase R61 by *N*-methoxybenzoyl-β-sultam (**4**) at pH 7.00 and 30 °C in 0.1 mol dm^{-3} MOPS buffer, $I = 1.0$ mol dm^{-3} (KCl), 6.93×10^{-8} mol dm^{-3} DD-peptidase R61, and 5.82×10^{-6} mol dm^{-3} *N*-methoxybenzoyl-β-sultam.

Table 2: Second-Order Rate Constants, k_{OH}, for Hydroxide Ion Catalyzed Hydrolysis and k_i for Inhibition of R61 at pH 7, 30 °C, and $I = 1.0$ mol dm^{-3} for *N*-Aroyl-β-sultams[a]

	N-aroyl-β-sultam			
	N-*p*-nitro (**6**)	*N*-*p*-chloro (**5**)	*N*-benzoyl (**3**)	*N*-*p*-methoxy (**4**)
k_{OH}/M^{-1} s^{-1}	5.18×10^4	2.08×10^4	1.38×10^4	8.99×10^3
k_i/M^{-1} s^{-1}	4.78×10^3	1.64×10^3	7.00×10^2	3.79×10^2

[a] Rate constants have an estimated error of ±3%.

time-dependent decrease in enzyme activity and tended toward zero with increasing *t*. If the enzyme was incubated alone under exactly the same conditions but in the absence of β-sultam, the observed activity remained constant throughout the experimental time frame. These control experiments were taken as 100% activity; the percentage activity of R61 activity remaining in the inhibitor experiments was calculated and plotted against *t*. This gave apparent first-order rate constants for inactivation (Figure 2), which showed a first-order dependence on the β-sultam concentration. The concentration of the enzyme is much lower than that of the inhibitor, and the rate of inactivation is effectively pseudo first order and so does not depend on the enzyme concentration. Second-order rate constants for inactivation, k_i, were obtained either by dividing the observed rate of inactivation by inhibitor concentration, k_{obs}/[I], when less than three inhibitor concentrations were used or graphically from slopes of the plots of the observed rate of inactivation against several inhibitor concentrations.

With some *N*-aroyl-β-sultams and at high pH there were problems with the accurate determination of rate constants for the inactivation process because of the competing base-catalyzed hydrolysis of these compounds. The actual concentration of β-sultam present was then calculated for each time period. The second-order rate constants k_i for the inactivation of R61 by various substituted β-sultams are given in Table 2.

Evidence for Active Site Sulfonylation. (a) pH Dependence of Inactivation. The *N*-benzoyl-β-sultam (**3**) is a time-dependent inhibitor of the R61 DD-peptidase, and its second-order rate constant for inactivation (k_i) varies with pH in a manner very similar to that of the second-order rate constant, k_{cat}/K_m, for the hydrolysis of the thioester substrate (**1** and **2**) catalyzed by R61 (Figure 1). This indicates that the rate of inactivation of R61 by this compound is controlled by the same catalytic groups in the active site that are used for substrate hydrolysis; i.e., active site-directed inhibition is occurring. The increase in enzyme activity toward inactivation with increasing pH is probably due to the deprotonation of Lys 65 or Tyr 159, as discussed earlier. Given that the inhibitor does not contain a carboxylic acid residue, this indicates that the observed ionization is due to the enzyme and not the substrate.

(b) ESIMS and X-ray Crystallography Data. Sulfonylation of the R61 enzyme by β-sultams as shown in Scheme 3 was confirmed by ESIMS. Samples of R61 inactivated by *N*-benzoyl-β-sultam (**3**) were subjected to ESIMS analysis; native R61 gave MW 37580 Da. Incubation of the enzyme with *N*-benzoyl-β-sultam (**3**) (MW 211 Da) showed a rapid formation of the sulfonylated adduct at 37791 Da corresponding to 1 mol of bound β-sultam.

X-ray crystallography revealed that ring opening of the β-sultam was part of the inactivation process (Figure 3). The structure, determined to 1.1 Å resolution, shows a sulfonate ester formed with Ser 62 Oγ. Interestingly, the inhibitor makes very few specific interactions with the enzyme active site. Indeed, most β-lactam compounds and peptide substrates make extensive interactions with residues in the enzyme's trough-like active site. *N*-Benzoyl-β-sultam hydrogen bonds to only three active site residues, including Tyr 159, Arg 285, and Thr 301 (Figure 3b). The interactions with the "roof" of the active site (*33*), dominated by Arg 285, are most likely crucial for initial binding of the inhibitor by the enzyme and for orienting the molecule for attack by Ser 62 Oγ. Another surprising aspect of this structure is that **3** does not bind in the oxyanion hole. To date, all compounds studied crystallographically with the R61 DD-peptidase have had an oxygen bound in the oxyanion hole formed by the main chain nitrogen atoms of Ser 62 and Thr 301. With peptide substrates, this interaction helps to polarize the scissile peptide bond, facilitating the peptidase reaction. Of course, it is possible that what is seen in the crystal structure is the result of a rearrangement, following ring opening. This has been observed in several crystal structures of analogous β-lactamases inhibited with β-lactam derivatives (*32*). The benzyl ring of the β-sultam does not make any interactions with the enzyme, and this is reflected in the less well defined density for this portion of the molecule. Modifying β-sultams with additional functionalities to allow more specific interactions with the enzyme active site will likely improve these compounds as DD-peptidase inhibitors.

In addition to the inhibitor molecule covalently bound to Ser 62 Oγ, there is a second molecule bound to the substrate specificity site of the active site (*33*). This region of the active site normally binds the glycine-L-diaminopimelic acid moiety of the natural cell wall peptide. In particular, two residues, Ser 326 and Asn 327, hydrogen bond with a carboxylate of this substrate. In the β-sultam-inhibited structure, two sulfate oxygens of a hydrolyzed molecule of *N*-benzoyl-β-sultam are fortuitously able to hydrogen bond to Ser 326 and Asn 327. As these are the only hydrogen-bonding interactions

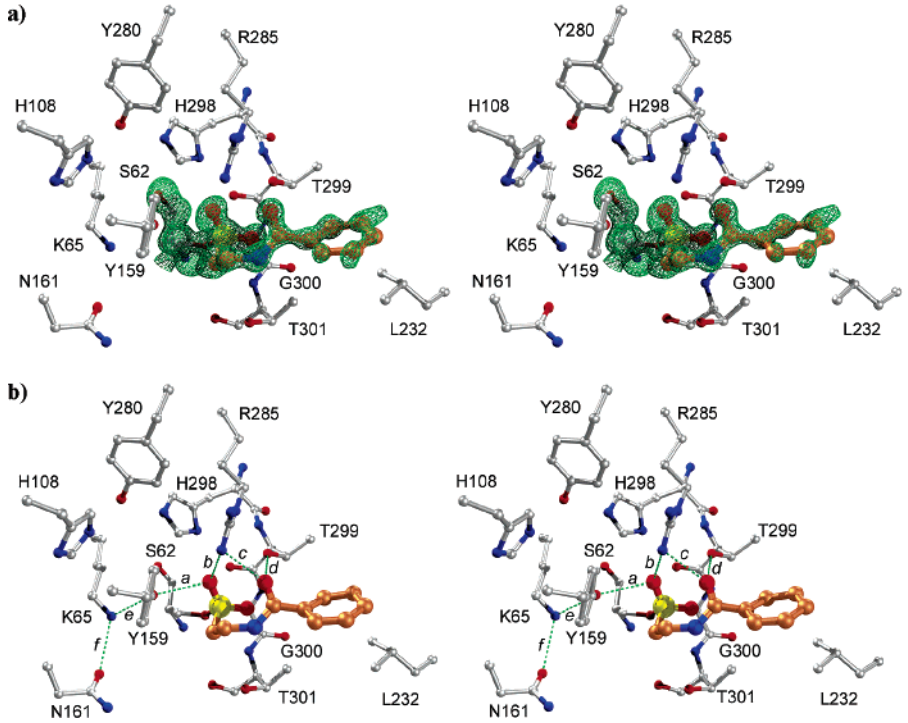

FIGURE 3: (a) Stereoview of the $|F_o| - |F_c|$ electron density map calculated with Ser 62 and the inhibitor (**3**) omitted from the model. The omit map is contoured at 3σ and clearly shows the sulfonylated acyl-enzyme, with *N*-benzoyl-β-sultam bound to the serine 62 Oγ. (b) Stereoview of the active site showing the interactions *N*-benzoyl-β-sultam makes with the R61 active site. The distances for these interactions are as follows: a, 3.0 Å; b, 3.0 Å; c, 2.7 Å; d, 2.5 Å; e, 2.7 Å; f, 3.0 Å. Both figures were created using PovScript (*38*) and rendered with PovRay.

Scheme 4

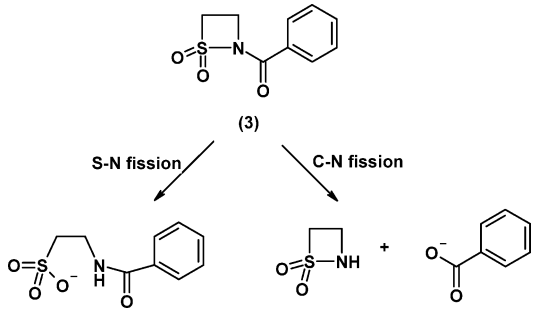

this second molecule of **3** makes with the enzyme, the inhibitor is clearly not being recognized by the species specificity site. Since the sulfonyl enzyme is shown to be stable for more than 4 weeks, we presume that the hydrolyzed molecule of **3** bound at the periphery of the active site ultimately derives from solvent-catalyzed hydrolysis of this rather labile compound.

N-Acylsulfonamides have been used previously to inactivate serine enzymes (*8*). However, the mechanism invariably involves acylation and C−N bond fission with the serine hydroxyl group attacking the amide to displace the sulfonamide as the leaving group. Although the β-sultams reported here are also formally *N*-acylsulfonamides, inactivation occurs by sulfonylation as a result of serine nucleophilic attack on the sulfonyl center and displacement of the amide as a leaving group, showing preferential S−N over C−N fission (Scheme 4).

(c) Catalysis of Sulfonyl Transfer. As active site-directed inhibition is occurring in the inactivation of R61 by *N*-benzoyl-β-sultam (**3**), it appears that the catalytic machinery of R61 is catalyzing the sulfonyl transfer process. This indicates a significant degree of flexibility within the enzyme as the stereochemical requirements for catalysis of a reaction involving sulfonyl transfer with a trigonal bipyramidal arrangement in the transition state are significantly different to acyl transfer reactions involving a tetrahedral intermediate. This is a similar situation to phosphoryl transfer reactions catalyzed by serine enzymes that are formally considered to catalyze only acyl transfer (*15*). For example, serine proteases possess an oxyanion hole, as does R61, which is used to stabilize the oxyanion in the tetrahedral intermediate (TI) formed after attack of the serine oxygen at a carbonyl center. This oxyanion will lie at ca. 109° to the newly formed serine O−C bond. In contrast, the oxyanion formed by attack at the β-sultam sulfonyl center is likely to occupy an equatorial position in a trigonal bipyramidal intermediate (TBPI) or transition state and will therefore lie at ca. 90° to the serine O−S bond. Although C−N bond fission in the hydrolysis of amides requires general acid catalysis to facilitate amine expulsion, the reactivity of *N*-acyl-β-sultams and their amide leaving groups may allow ring opening to occur without N-protonation. The catalysis of sulfonyl transfer from the β-sultam to the active site serine of R61 may therefore only be possible because ring opening occurs in a single step without general acid catalysis (Scheme 3) (*13*).

(d) Reactivation. The inactivation of the R61 enzyme is irreversible, and the resulting sulfonyl enzyme is stable for up to 4 weeks in the incubation solution at 30 °C. By contrast for some serine proteases, such as α-chymotrypsin, inactivated by sulfonyl fluorides (*16*, *34*), it is possible to reactivate the enzyme above pH 8.5 (*35*). The sulfonyl R61 enzyme inactivated by *N*-benzoyl-β-sultam was not reactivated by treatment with hydroxylamine and showed no evidence of mass loss by ESIMS.

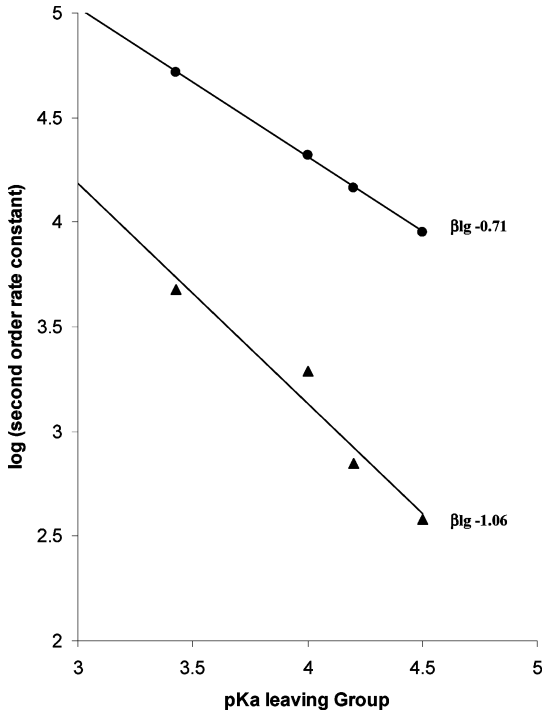

FIGURE 4: Brönsted plots for *N*-aroyl-β-sultams: alkaline hydrolysis, k_{OH} (●), and R61 inhibition, k_i (▲).

(e) Structure–Activity Relationships. The fact that the β-sultam has ring opened upon inactivation of the enzyme confirms the necessity of S–N fission for activity. However, it is important to separate the effects of substituents on chemical reactivity and molecular recognition. For example, N-substituents not only influence the rate of S–N bond fission and reaction through inductive effects, altering the electrophilicity of the sulfonyl center, N-basicity, and amine nucleofugacity, but also change binding energies through molecular recognition effects such as interactions between the substituent and a binding pocket in the enzyme. The least effective R61 inhibitor in the simple *N*-aroyl-β-sultams is also the least reactive, the *N*-*p*-methoxybenzoyl compound (**4**) with a k_{OH} of 8.99×10^3 M^{-1} s^{-1}. A comparison of the k_i values at pH 7 with the second-order rate constants for hydroxide ion hydrolysis, k_{OH} values (Table 2), for the N-aroylated compounds indicates that their relative effectiveness as R61 inhibitors is largely due to variations in their chemical reactivity.

The effect of changing the basicity of the leaving group in β-sultams on the rate of inactivation of R61 was investigated by different aryl substituents in *N*-aroyl-β-sultams. The second-order rate constants for inactivation, k_i, for a series of substituted derivatives are given in Table 2. Electron-withdrawing substituents in the *N*-aroyl residue increase the rate of inactivation. These constants give an opportunity to use linear free energy relationships to help to elucidate the reaction mechanism and the transition state structure. Although the pK_as of the amide leaving groups are not known, those of the corresponding carboxylic acids are readily available. A Brönsted-type plot of the logarithm of k_i against the pK_a of the analogous carboxylic acid is shown in Figure 4, the slope of which gives a Brönsted β_{lg} of −1.06. This value is indicative of a development of a significant negative charge on the amide nitrogen leaving group compared with the relative positive effective charge

Scheme 5

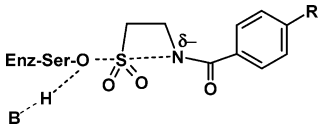

of at least 0.7+ on the nitrogen in the reactant (*36*). It suggests the leaving group is expelled as the amide anion and that S–N bond fission is almost complete in the transition state (Scheme 5).

The second-order rate constants, k_{OH}, for the alkaline hydrolysis of the same series of *N*-aroyl-β-sultams are also given in Table 2. The corresponding Brönsted-type plot for these values generates a β_{lg} of −0.71 (Figure 4), indicative of much less change in charge on the leaving nitrogen in the transition state. If a trigonal bipyramidal intermediate is formed in the alkaline hydrolysis of *N*-aroyl-β-sultams (*37*) and if the rate of S–N bond fission and ring opening to expel the amide anion is greater than the rate of expulsion of hydroxide ion from the intermediate, then formation of the intermediate will be rate limiting. For *N*-aroyl-β-sultams N-protonation of the leaving group amide is thermodynamically unfavorable and amide anion expulsion could occur, but at a rate which is comparable or even slower than that for hydroxide ion. Therefore, breakdown of the intermediate may become rate limiting.

Compared with the base-catalyzed hydrolysis of *N*-aroyl-β-sultams by hydroxide ion, the R61 enzyme reaction appears to cause a move to a transition state later along the reaction coordinate. The different Brönsted β_{lg} values indicate considerably more S–N bond fission in the transition state for the enzyme-catalyzed reaction. The enzyme appears to be using some of its catalytic machinery to facilitate the sulfonylation reaction, but presumably the geometry of the displacement reaction is not ideal. The host of favorable noncovalent interactions, evolved by the enzyme to stabilize the transition state for the "natural" substrate, is not fully available to lower the activation energy for the β-sultams, and so the transition state occurs later along the reaction coordinate.

The rates of enzyme inactivation observed could be increased if recognition elements are built into the structure of the β-sultams. β-Sultams (**3**–**6**) are far from ideal as R61 inhibitors as they are relatively hydrolytically labile. Suitable substituents could improve binding to R61 and hence increase the rate of inactivation of the serine residue. Second, they may reduce the hydrolytic lability of the inhibitor, thus making it more stable in aqueous solution and in a biological environment.

In conclusion, *N*-aroyl-β-sultams are a novel class of inhibitor compounds that inactivate serine enzymes by irreversible sulfonylation of the active site serine residue. They are inactive toward enzymes lacking active serine residues, such as the metallo-β-lactamases, indicating that specific sulfonylation of active site residues takes place.

SUPPORTING INFORMATION AVAILABLE

Synthesis of the substrates *N*-benzoyl-D-Ala-thio-D-lactate (**1**) and *N*-benzoyl-D-Ala-thioglycolate (**2**). This material is available free of charge via the Internet at http://pubs.acs.org.

REFERENCES

1. Spratt, B. G. (1975) Distinct penicillin binding proteins involved in the division elongation and shape of *Escherichia coli* K12, *Proc. Natl. Acad. Sci. U.S.A. 72*, 2999−3003.
2. Koch, A. L. (2000) Penicillin binding proteins, β-lactams, and lactamases: offensives attacks, and defensive countermeasures, *Crit. Rev. Microbiol. 26*, 205−220.
3. Ghuysen, J. M. (1991) Serine beta-lactamases and penicillin-binding proteins, *Annu. Rev. Microbiol. 45*, 37−67.
4. Goffin, C., and Ghuysen, J. M. (2002) Biochemistry and comparative genomics of SxxK superfamily acyltransferases offer a clue to the mycobacterial paradox: presence of penicillin-susceptible target proteins versus lack of efficiency of penicillin as therapeutic agent, *Microbiol. Mol. Biol. Rev. 66*, 702−738.
5. Tipper, D. J., and Strominger, J. L. (1965) Mechanism of action of penicillins: a proposal based on their structural similarity to acyl-D-alanyl-alanine, *Proc. Natl. Acad. Sci. U.S.A. 54*, 1133−1141.
6. Kelly, J. A., Dideberg, O., Charlier, P., Wery, J.-P., Libert, M., Moews, P. C., Knox J. R., Duez, C., Fraipont, C., Joris, B., Dusart, J., Frère, J.-M., and Ghuysen, J.-M. (1986) On the origin of bacterial resistance to penicillin: comparison of a β-lactamase and a penicillin target, *Science 231*, 1429−1431.
7. Massova, I., and Mobashery, S. (1999) Structural and mechanistic aspects of evolution of beta-lactamases and penicillin-binding proteins, *Curr. Pharm. Des. 5*, 929−937.
8. Anderson, J. W., and Pratt, R. F. (2000) Dipeptide binding to the extended active site of the *Streptomyces* R61 D-alanyl-D-alanine peptidase: The path to a specific substrate, *Biochemistry 39*, 12200−12209.
9. Frère, J.-M., and Joris, B. (1985) Penicillin-sensitive enzymes in peptidoglycan biosynthesis, *CRC Crit. Rev. Microbiol. 11*, 299−396.
10. Kelly, J. A., Knox, J. R., Moews, P. C., Hite, G. J., Bartolone, J. B., Zhao, H., Joris B., Frère, J.-M., and Ghuysen, J.-M. (1985) 2.8Å Structure of penicillin-sensitive D-alanylcarboxypeptidase-transpeptidase from *Streptomyces* R61 and complexes with β-lactams, *J. Biol. Chem. 260*, 6449−6458.
11. Jamin, M., Adam, M., Damblon, C., Christiaens, L., and Frère, J.-M. (1991) Accumulation of acyl-enzyme in DD-peptidase-catalysed reactions with analogues of peptide substrates, *Biochem. J. 280*, 499−506.
12. Kiener, P. A., and Waley, S. G. (1978) Reversible inhibitors of penicillinases, *Biochem. J. 169*, 197−204; Beesley, T., Gascoyne, N., Knott-Hunziker, V., Petursson, S., Waley, S. G., Jaurin, B., and Grunstrom, T. (1983) The inhibition of class C beta-lactamases by boronic acids, *Biochem. J. 209*, 229−233; Crompton, I. E., Cuthbert, B. K., Lowe, G., and Waley, S. G. (1988) Beta-lactamase inhibitors. The inhibition of serine beta-lactamases by specific boronic acids, *Biochem. J. 251*, 453−459; Ness, S., Martin, R., Kindler, A. M., Paetzel, M., Gold, M., Jensen, S. E., Jones, J. B., and Strynadka, N. C. (2000) Structure-based design guides the improved efficacy of deacylation transition state analogue inhibitors of TEM-1 beta-Lactamase, *Biochemistry 39*, 5312−5321; Powers, R. A., Blazquez, J., Weston, G. S., Morosini, M. I., Baquero, F., and Shoichet, B. K. (1999) The complexed structure and antimicrobial activity of a non-beta-lactam inhibitor of AmpC beta-lactamase, *Protein Sci. 8*, 2330−2337.
13. Pratt, R. F. (1989) Inhibition of a class C β-lactamase by a specific phosphonate monoester, *Science 246*, 917−919; Rahil, J., and Pratt, R. F. (1991) Phosphonate monoester inhibitors of class A beta-lactamases, *Biochem. J. 275*, 793−795; Rahil, J., and Pratt, R. F. (1992) Mechanism of inhibition of the class C beta-lactamase of *Enterobacter cloacae* P99 by phosphonate monoesters, *Biochemistry 31*, 5869−5878; Rahil, J., and Pratt, R. F. (1993) Structure−activity relationships in the inhibition of serine beta-lactamases by phosphonic acid derivatives, *Biochem. J.* 296, 389−393; Lobkovsky, E., Billings, E. M., Moews, P. C., Rahil, J., Pratt, R. F., and Knox, J. R. (1994) Crystallographic structure of a phosphonate derivative of the *Enterobacter cloacae* P99 cephalosporinase: mechanistic interpretation of a beta-lactamase transition-state analog, *Biochemistry 33*, 6762−6772; Rahil, J., and Pratt, R. F. (1994) Characterization of covalently bound enzyme inhibitors as transition-state analogs by protein stability measurements: phosphonate monoester inhibitors of a beta-lactamase, *Biochemistry 33*, 116−125; Kaur, K., Lan, M. J., and Pratt, R. F. (2001) Mechanism of inhibition of the class C beta-lactamase of *Enterobacter cloacae* P99 by cyclic acyl phosph(on)ates: rescue by return, *J. Am. Chem. Soc. 123*, 10436−10443; Kaur, K., Adediran, S. A., Lan, M. J.,and Pratt, R. F. (2003) Inhibition of beta-lactamases by monocyclic acyl phosph(on)ates, *Biochemistry 42*, 1529−1536; Nagarajan, R., and Pratt, R. F. (2004) Thermodynamic evaluation of a covalently bonded transition state analogue inhibitor: inhibition of β-lactamases by phosphonates, *Biochemistry 43*, 9664−9673.
14. Baxter, N. J., Laws, A. P., Rigoreau, L., and Page, M. I. (1996) The hydrolytic reactivity of β-sultams, *J. Chem. Soc., Perkin Trans. 2*, 2245−2246.
15. Beardsell, M., Hinchliffe, P. S., Wood, J. M., Wilmouth, R. C., Schofield, C. J., and Page, M. I. (2001) β-Sultams−A novel class of serine protease inhibitors, *Chem. Commun.*, 497−498.
16. Hinchliffe, P. S., Wood, J. M., Davis, A. M., Austin, R. P., Beckett, R. P., and Page, M. I. (2003) Structure−reactivity relationships in the inactivation of elastase by β-sultams, *Org. Biomol. Chem. 1*, 67−80.
17. Lee, W., McDonough, M. A., Kotra, L., Li, Z. H., Silvaggi, N. R., Takeda, Y., Kelly, J. A., and Mobashery, S. (2001) A 1.2Å snapshot of the final step of bacterial cell wall biosynthesis, *Proc. Natl. Acad. Sci. U.S.A. 98*, 1427−1431.
18. Silvaggi, N. R., Anderson, J. W., Brinsmade, S. R., Pratt, R. F., and Kelly, J. A. (2003) Crystal structure of phosphonate-inhibited D-Ala-D-Ala peptidase reveals an analog of a tetrahedral transition state, *Biochemistry 42*, 1199−1208.
19. Silvaggi, N. R., Kaur, K., Adediran, S. A., Pratt, R. F., and Kelly J. A. (2004) Toward better antibiotics: crystallographic studies of a novel class of DD-peptidase/beta-lactamase inhibitors, *Biochemistry 43*, 7046−7053.
20. Kuzin, A. P., Liu, H., Kelly, J. A., and Knox, J. R. (1995) Binding of cephalothin and cefotaxime to D-ala-D-ala peptidase reveals a functional basis of a natural mutation in a low-affinity penicillin-binding protein and in extended-spectrum β-lactamases, *Biochemistry 34*, 9532−9540.
21. Frère, J.-M., Leyh-Bouille, M., Ghuysen, J.-M., Nieto, M., and Perkins, H. R. (1976) Extracellular DD-carboxypeptidases-transpeptidases from *Streptomyces*, *Methods Enzymol. 45*, 610−636.
22. Champseix, A., Chanet-Ray, J., Ettienne, A., Le Berre, A., Masson, J., Napierale, C., and Vessiere, R. (1985) Synthèses de β-sultames (thiazétidines-1,2 dioxyde-1,1), *Bull. Soc. Chim. Fr. 3*, 463−472.
23. Dean, J. A., Ed. (1973) *Lange's Handbook of Chemistry*, 11 ed., pp 5−7, McGraw-Hill, New York.
24. Kelly, J. A., Knox, J. R., Zhao, H., Frère, J.-M., and Ghuysen, J.-M. (1989) Crystallographic mapping of β-lactams bound to a D-alanyl-D-alanine peptidase target enzyme, *J. Mol. Biol. 209*, 281−295.
25. Otwinowski, Z., and Minor, W. (1997) Processing of X-ray diffraction data collected in oscillation mode, *Methods Enzymol. 276*, 307−326.
26. Brünger, A. T., Adams, P. D., Clove, G. M., Delano, W. L., Gros, P., Grosse-Kunstleve, R. W., Jiang, J.-S., Kuszewski, J., Nilges, M., Pannu, N. S., Read, R. J., Rice, L. M., Simonson, T., and Warren, G. L. (1998) Crystallography and NMR system: A new software suite for macromolecular structure determination, *Acta Crystallogr. D54*, 905−921.
27. Sheldrick, G. M., and Schneider, T. R. (1997) SHELXL: high-resolution refinement, *Methods Enzymol. 277*, 319−343.
28. McRee, D. E. (1999) XtalView/Xfit−A versatile program for manipulating atomic coordinates and electron density, *J. Struct. Biol. 125*, 156−165.
29. Moews, P. C., Knox, J. R., Dideberg, O., Charlier, P., and Frère, J.-M. (1990) The structure of the β-lactamase of *Bacillus licheniformis* 749/C at 2.0Å resolution, *Proteins: Struct., Funct., Genet. 7*, 156−171.
30. Massova, I., and Mobashery, S. (1998) Kinship and diversification of bacterial penicillin-binding proteins and β-lactamases, *Antimicrob. Agents Chemother. 42*, 1−17.
31. Varetto, L., Frère, J.-M., Nguyen-Disteche, M., Ghuysen, J.-M., and Houssier, C. (1987) The pH dependence of the active-site serine DD-peptidase of *Streptomyces* R61, *Eur. J. Biochem. 162*, 525−531.
32. Fisher, J. F., Meroueh, S. O., and Mobashery, S. (2005) Bacterial resistance to β-lactam antibiotics: compelling opportunism, compelling opportunity, *Chem. Rev. 105*, 395−424.
33. McDonough, M. A., Anderson, J. W., Silvaggi, N. R., Pratt, R. F., Knox, J. R., and Kelly, J. A. (2002) Structures of two kinetic intermediates reveal species specificity of penicillin binding proteins, *J. Mol. Biol. 322*, 111−122.

34. Fahrney, D. E., and Gold, A. M. (1963) Sulfonyl fluorides as inhibitors of esterases. I. Rates of reaction with acetylcholinesterase, α-chymotrypsin and trypsin, *J. Am. Chem. Soc. 85*, 997−1000; Turini, P., Kurooka, S., Steer, M., Corbascio, A. M., and Singer, T. P. (1967) The action of phenylmethysulfonyl fluoride on human acetylcholinesterase, chymotrypsin and trypsin, *J. Pharm. Exp. Ther. 167*, 98−104; Lawrence, J. B. (1972) Urea denaturation of active-site spin-labeled α-chymotrypsin, *Biochemistry 11*, 2921−2924; Lawrence, J. B., and Shan, S. W. (1974) Spin-labeled sulfonyl fluorides as active site probes of protease structure. I. Comparison of the active site environments in α-chymotrypsin and trypsin, *J. Biol. Chem. 249*, 1668−1677; Hideaki, T., Hiroyasu, N., and Lawrence, J. B. (1984) Synthesis and evaluation of 19-F labelled sulfonyl fluorides as probes of protease structure: α-chymotrypsin, *Biochem. J. 96*, 349−355.

35. Gold, A. M., and Fahrney, D. (1964) Sulfonyl fluorides as inhibitors of esterases. II. Formation and Reactions of phenylmethanesulfonyl alpha-chymotrypsin, *Biochemistry 3*, 783−791.

36. Page, M. I., and Williams, A. (1997) in *Organic and Bio-organic Mechanisms*, pp 52−80, Longmans, Harlow.

37. Baxter, N. J., Laws, A., Rigoreau, L. J. M., and Page, M. I. (2000) Reactivity and mechanism in the hydrolysis of β-sultams, *J. Am. Chem. Soc. 122*, 3375−3385.

38. Kraulis, P. J. (1991) *J. Appl. Crystallogr. 24*, 946−950; Fenn, T. D., Ringe, D., and Petsko, G. A. (2003) *J. Appl. Crystallogr. 36*, 944−947.

BI050110O